

Phase Mapping Ni-based alloys with EBSD Using Deep Learning

Alfred Yan¹, Gabriel Trindade Dos Santos¹, Ramandeep Mandia¹, Roberto dos Reis¹, Vinayak P. Dravid¹

¹ Department of Materials Science and Engineering, Northwestern University, Evanston, IL, United States.

Abstract

Electron Backscattered Diffraction (EBSD) is a diffraction modality in the Scanning Electron Microscopy (SEM) that can collect a map of Diffraction Patterns (DP) from a region in a sample. The DP contains a variety of information about the sample, including the orientation, crystallography, and defect contrast ¹. Phase mapping is also a useful application for EBSD, and convolutional neural networks (CNNs) can be used to rapidly identify the material phase from a DP. Some past CNN-based workflows have demonstrated the ability to identify subtle differences in composition and compositional ordering from an EBSD pattern using neural networks, which would otherwise be impossible with conventional techniques ². With this capability, we evaluate the performance of neural networks for classifying patterns into Ni-based alloy phases using both cross entropy and contrastive training.

Methods and Results

EBSD patterns are acquired from the literature from the phases fcc Ni, L1₂ Ni₃Al, and L1₂ Ni₃Fe³, which have relevant applications in high-temperature and corrosion resistance⁴. The L1₂ structures contain a base fcc structure with compositional ordering of the two constituent elements. Due to the similarity in crystal structures, differentiation between these phases is expected to be challenging.

Next, neural networks are trained to classify Kikuchi patterns into one of the phases. Similarity-based contrastive learning⁵ has shown some promise at supervised classification tasks, but has not been demonstrated for phase mapping in EBSD. Thus, this project compares supervised contrastive learning with convolutional neural networks trained with standard cross-entropy loss. First, a CNN with the EfficientNet architecture was trained for 14 epochs using cross entropy loss. Random horizontal and vertical flips were used for data augmentation. Afterwards, a CNN with the same architecture, data augmentation, and optimizer was trained using contrastive loss. The contrastive loss function was used, which minimizes the distance between embeddings from different images in the same class, while increasing it between embeddings from different classes whose distances are less than a specific margin⁵. In our implementation, the L_p distance was used. Training was also done for 14 epochs.

Patterns from these phases were split into train, validation, and test sets. The test data was ensured to have been collected from different areas of the sample from the training data. The models were first trained on the training data and evaluated on the validation data. Then, it was retrained on both the training and validation data and evaluated on the test data. The validation and test accuracies are displayed in Figure 1. Both contrastive and cross entropy learning achieve approximately equivalent performances, although this may fluctuate with more

hyperparameter tuning, such as increasing the number of epochs. The cross-entropy loss results showed a spike in test accuracy at early epochs, indicating some overfitting, possible due to the small dataset size. Additionally, the high validation scores compared to the test scores likely arise from the patterns originating from the same scanned area as the training patterns, which also causes some overfitting.

A confusion matrix was created from the cross entropy model predictions, shown in Figure 2. Ni and Ni₃Fe were often misclassified, which is likely due to the low difference in atomic number between Fe (26) and Ni (28). This suggests a physical limit to the composition information obtainable from EBSD patterns. However, the overall performance for the three phases still reinforce the potential for improved phase mapping over conventional techniques that only analyze band geometries.

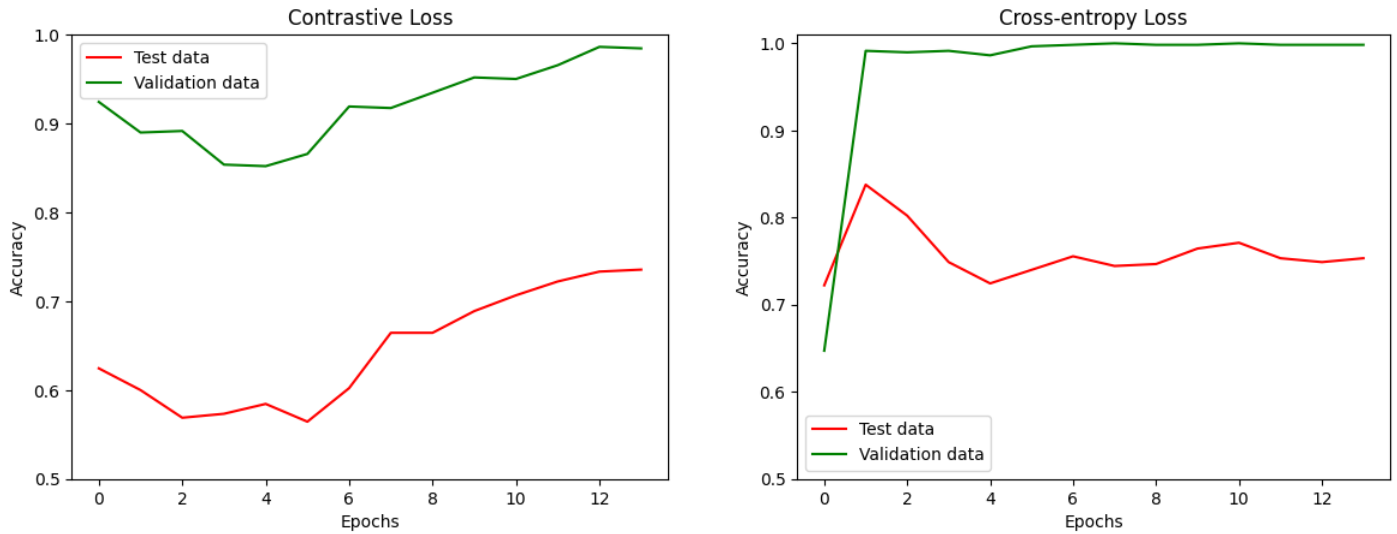


Figure 1: Validation and test accuracies for both contrastive learning and cross entropy learning.

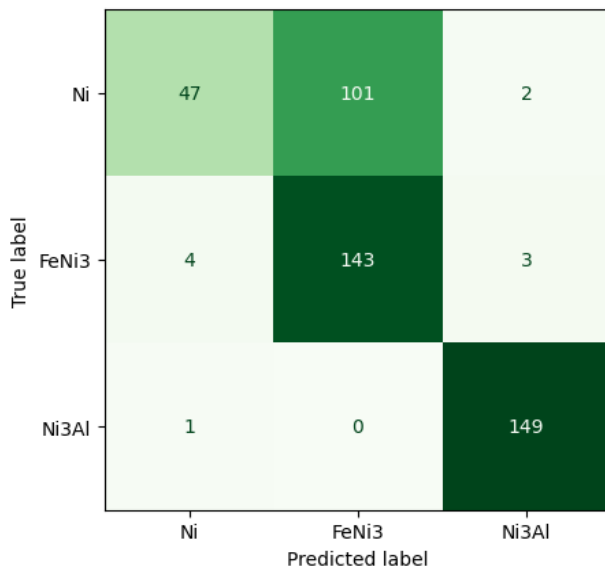


Figure 2: Confusion matrix showing model predictions from the model trained using cross entropy loss.

Acknowledgements: This research was supported in part through the computational resources and staff contributions provided for the Quest high performance computing facility at Northwestern University which is jointly supported by the Office of the Provost, the Office for Research, and Northwestern University Information Technology. This work made use of Northwestern University's NUANCE Center, which has received support from the SHyNE Resource (NSF ECCS-2025633), the International Institute for Nanotechnology (IIN), and Northwestern's MRSEC program (NSF DMR-2308691).

References:

- (1) della Ventura, N. M.; Lamb, J. D.; Lenthe, W. C.; Echlin, M. P.; Pürstl, J. T.; Trageser, E. S.; Quevedo, A. M.; Begley, M. R.; Pollock, T. M.; Gianola, D. S.; De Graef, M. Orientation-Adaptive Virtual Imaging of Defects Using EBSD. *Ultramicroscopy* **2025**, 276, 114205. <https://doi.org/10.1016/j.ultramic.2025.114205>.
- (2) Kaufmann, K.; Zhu, C.; Rosengarten, A. S.; Maryanovsky, D.; Wang, H.; Vecchio, K. S. Phase Mapping in EBSD Using Convolutional Neural Networks. *Microscopy and Microanalysis* **2020**, 26 (3), 458–468. <https://doi.org/10.1017/S1431927620001488>.
- (3) Kaufmann, K.; Zhu, C.; Rosengarten, A. S.; Vecchio, K. S. Deep Neural Network Enabled Space Group Identification in EBSD. *Microscopy and Microanalysis* **2020**, 26 (3), 447–457. <https://doi.org/10.1017/S1431927620001506>.
- (4) *High-temperature site preference and atomic short-range ordering characteristics of ternary alloying elements in γ'-Ni₃Al intermetallics: Philosophical Magazine: Vol 97 , No 29 - Get Access.* <https://www.tandfonline.com/doi/full/10.1080/14786435.2017.1344787> (accessed 2025-12-18).
- (5) Musgrave, K.; Belongie, S.; Lim, S.-N. PyTorch Metric Learning. arXiv August 20, 2020. <https://doi.org/10.48550/arXiv.2008.09164>.